# Chemical Synthesis, Refolding, and Characterization of Mirror-Image Cyclophilin A

Ahmet Yesilcimen,[1#] Satish Gandhesiri,[1#] Tara L. Travaline,[2] Alex J. Callahan,[1] Olena S. Tokareva,[2] Andrei Loas,[1] John H. McGee,[2*] Bradley L. Pentelute[1,3,4,5*]

[1] Department of Chemistry, Massachusetts Institute of Technology, 77 Massachusetts Avenue, Cambridge, MA 02139, USA
[2] FOG Pharmaceuticals Inc., 30 Acorn Park Drive, Cambridge, MA 02140, USA
[3] The Koch Institute for Integrative Cancer Research, Massachusetts Institute of Technology, 500 Main Street, Cambridge, MA 02142, USA
[4] Center for Environmental Health Sciences, Massachusetts Institute of Technology, 77 Massachusetts Avenue, Cambridge, MA 02139, USA
[5] Broad Institute of MIT and Harvard, 415 Main Street, Cambridge, MA 02142, USA

[#] Equal contribution
* To whom correspondence should be addressed: jmcgee@fogpharma.com, blp@mit.edu

**Abstract:** The chemical synthesis of proteins (CSP) has been an essential tool in studying and understanding the role of these biological polymers and enabling the discovery of novel classes of inhibitors. However, CSP with commercially available synthesizers is typically limited to producing polypeptides of about 50 to 70 amino acids in length. Consequently, a wide range of protein targets have been out of reach using these technologies or require cumbersome synthesis and purification of multiple peptide fragments. In this report, we employed a powerful combination of automated flow peptide synthesis (AFPS), native chemical ligation (NCL) techniques, and high-throughput evaluation of refolding conditions to achieve the first chemical synthesis of both the wild-type and mirror-image forms of functional full-length CypA protein, which plays a vital role in proline cis-trans isomerization and other important processes. Functional assays confirmed that the chemically synthesized proteins retained their biological properties.

## Introduction

Cyclophilin A (CypA), a member of the cyclophilin protein family, has captured the interest of the scientific community due to its crucial role as a peptidyl-prolyl isomerase (PPI) enzyme.[1] This protein, which is ubiquitous across various tissues and cellular environments, is integral to numerous biological processes.[1–5] CypA primarily acts as an essential component in protein folding and assembly, facilitating the conversion between cis and trans isomers of peptidyl-prolyl bonds, thus ensuring the correct protein conformation.[6] Additionally, CypA has been identified as a crucial element in immune responses and inflammation. It interacts with important molecules in immune signaling pathways, including calcineurin and the T-cell receptor, particularly in the presence of cyclosporin A.[7] These interactions place CypA at the nexus of regulating complex signaling cascades.[1] Furthermore, recent studies have shown that when the molecular surface of CypA is remodeled by small-molecule ligands it is capable of targeting the active state of KRASG12C.[8,9] The broad range of functionalities and molecular interactions of CypA underscores its profound importance in cellular physiology and its potential as a promising therapeutic target for a diverse spectrum of pathological conditions, including autoimmune diseases and viral infections, and cancer.[1–8]

In the past few decades, chemical protein synthesis (CPS) has evolved into a formidable and adaptable tool in chemical biology and drug discovery.[10–15] CPS offers numerous advantages, facilitating the production and systematic exploration of difficult-to-access proteins enabled by the significant advancements in ligation chemistry, and flow synthesis.[10,13,16,17] These innovations have broadened the scope of CPS and enabled easy access to modified proteins with tailored properties and functionalities.[18,19] For instance, using CPS to synthesize mirror-image proteins could offer significant potential in identifying protease-stable peptide-based probes by utilizing a mirror-image phage display platform.[20–25] By leveraging this innovative strategy, researchers can obtain deeper insights into complex biological mechanisms, setting the stage for the development of groundbreaking therapeutics.[25] The ongoing advancements in CPS and the exploration of mirror-image proteins have the potential to significantly influence drug discovery and deepen our comprehension of fundamental biological phenomena.

## Results and Discussion

Our team recently introduced an innovative approach that uses automated fast-flow technology for synthesizing a wide range of protein chains in a continuous, stepwise 'single-shot' process.16 Our initial attempt to achieve the synthesis of the full-length CypA protein that is comprised of 166 amino acid residues using automated-flow peptide synthesis (AFPS) did not afford the desired protein chain. Further, the liquid chromatography-mass spectrometry (LC-MS) analysis of the unpurified reaction mixture after cleavage revealed that this strategy resulted in the generation of a complex reaction mixture consisting of various side products including single or multiple amino acid deletions, methionine oxidation, and truncated peptides (Figure 1A and SI Section 4.1).[26–28]

In light of these challenges, we developed an approach that integrates AFPS and native chemical ligation (NCL) strategies to successfully synthesize full-length CypA protein, while substituting methionine residues with norleucine (Nle) to mitigate the apparent oxidation issue (Figures 1B and 2).28 Of the four cysteine (Cys) residues in the sequence, we strategically chose

to perform the NCL reaction at the junction between Nle-62 and Cys-63 due to its favorable positioning and reaction kinetics.[29] Thus, we proposed the synthesis of full-length CypA by independently synthesizing and purifying two fragments: the N-

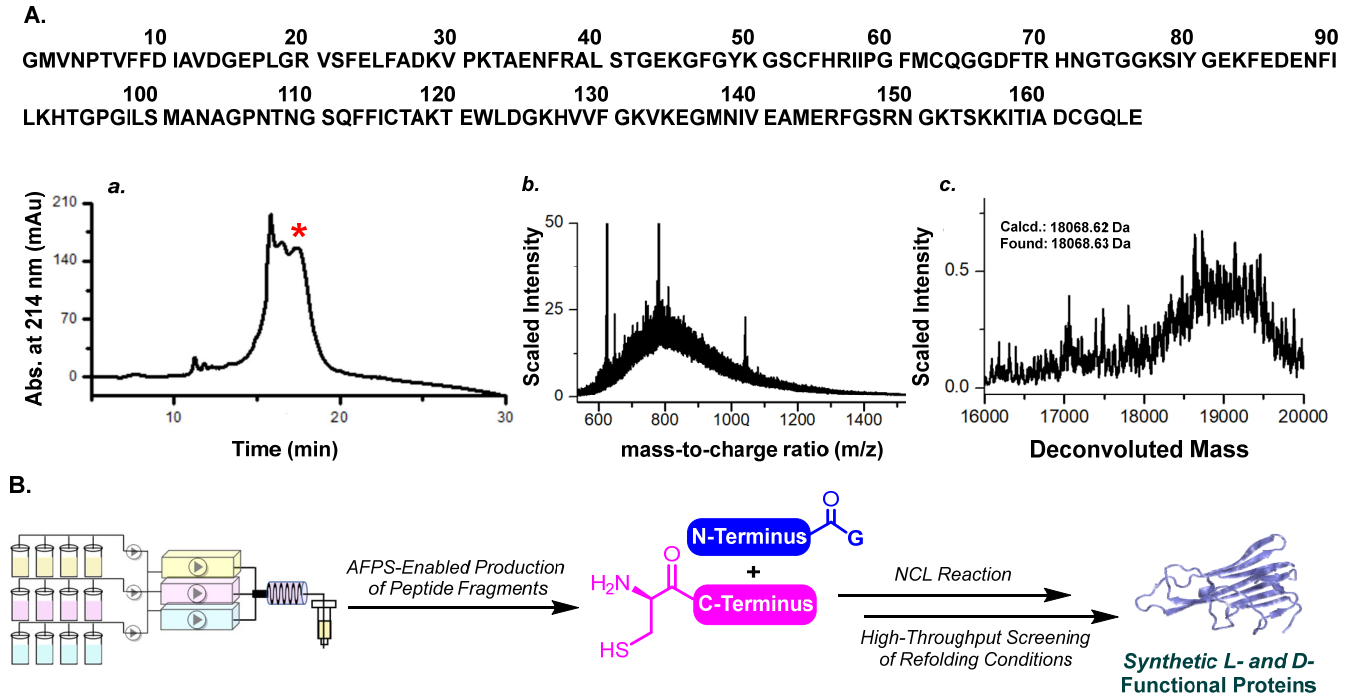


**Figure 1.** Automated fast-flow peptide synthesis (AFPS) enables access to synthetic full-length proteins. **A.** Amino acid sequence of full-length human CypA and single-shot synthesis of full-length CypA using AFPS. Shown are characterizations of the unpurified reaction mixture of full-length L- CypA by RP-HPLC using UV detection at 214 nm (***a***), the mass-to-charge spectrum of the total ion current post-injection on a Q-TOF LC-MS instrument (***b***), and the deconvolution mass spectrum analysis (***c***). The asterisk (*) in the analytical HPLC spectrum marks the primary product peak, which corresponds to the integrated mass-to-charge and deconvoluted mass spectra shown in (***b***) and (***c***). **B.** Our group has demonstrated a synthetic approach that leverages both AFPS, NCL, and high-throughput screening of refolding conditions for the production of elusive full-length proteins. "G" represents a thiol-reactive leaving group that is typically utilized in NCL reactions.

terminal fragment (residues 1–62, Figure 2) which presented a Dawson linker,[30] and the C-terminal fragment (residues 63–166) using AFPS technology and fluorenylmethyloxycarbonyl (Fmoc)-based solid-phase peptide synthesis strategies.[31] Further, a biotin tag was incorporated at the Gly-1 residue, enabling the resulting protein to be used in affinity selection-based discovery platforms to identify novel ligands for CypA protein.

The synthesis of the N-terminal fragment featuring 3-amino-4-(methylamino)benzamide (MeDbz) was highly efficient. To activate the MeDBz group, the N-terminal fragment was treated with 4-nitrophenyl chloroformate and N,N-Diisopropylethylamine, resulting in the activated N-terminal fragment possessing N'-methyl-benzimidazolinone (MeNbz).[32] Upon activation, the peptide fragment was cleaved from the resin using trifluoroacetic acid (TFA)-based cleavage cocktails (see SI Section2 for details).[33] Subsequently, the crude reaction mixture was purified by reverse-phase HPLC (RP-HPLC) to afford 7.4 mg of the purified N-terminal fragment (3.7% overall yield, Figure 2C and S4). In contrast, the synthesis of the C-terminal fragment proved less efficient. Despite this challenge, we were able to obtain the purified peptide in 4.5 mg quantity after cleaving the peptide chain from the solid support and subsequently purifying it using RP-HPLC (1.6% overall yield, Figure 2C and S6).

The NCL reaction between the purified N-terminus and the C-terminus successfully delivered the full-length CypA protein (Figure 3A). Specifically, 4.5 mg of N-terminus featuring a MeNbz unit (0.55 μmol), was dissolved in an NCL buffer (6.0 M Gdm•HCl, 200 mM NaPi, 44 mM 4-mercaptophenylacetic acid (MPAA), 22 mM Tris(2-carboxyethyl)phosphine hydrochloride (TCEP), pH = 7.2) to form a 3.0 mM peptide solution. Meanwhile, in a separate tube, 1.2 equivalent of purified C-terminal fragment (0.66 μmol) was dissolved using the same ligation buffer under an inert atmosphere. Once dissolved, these solutions were mixed and the resulting solution was placed in a 37 ºC water bath. Remarkably, the reaction reached completion within 4 hours, with some N-terminus hydrolysis side products observed.

The solubility difference between full-length CypA, and other species in the reaction mixture enabled the development of a rapid purification approach. Traditionally, the purification of ligated products necessitates laborious HPLC purification procedures, often resulting in handling losses and low yields.[30] During our investigation, it was discovered that the full-length CypA protein chain is more hydrophobic than its components (i.e., CypA N-terminus and C-terminus). To exploit this property, the NCL reaction mixture was diluted with 4 ºC water (30-fold) and rapidly frozen using liquid nitrogen. The frozen sample was then incubated at 37 ºC until it was thawed into a cloudy mixture, which was centrifuged at 4000 rpm for 10 minutes to form a pellet. Remarkably, this pellet predominantly contained the desired full-length ligated product (purity level ≈ 70% by RP-HPLC), with a minor presence of the N-terminal hydrolysis product. To further refine the pellet, it was dissolved in a mixture of acetonitrile and water (1:1) containing 0.1% TFA, followed by freeze-drying overnight. The resulting lyophilized powder, containing both the ligated product and the N-terminal hydrolysis

product, was then directly transitioned to the folding step without requiring additional purification.

High-throughput evaluation of a wide range of refolding buffers using the differential scanning fluorimetry (DSF) platform

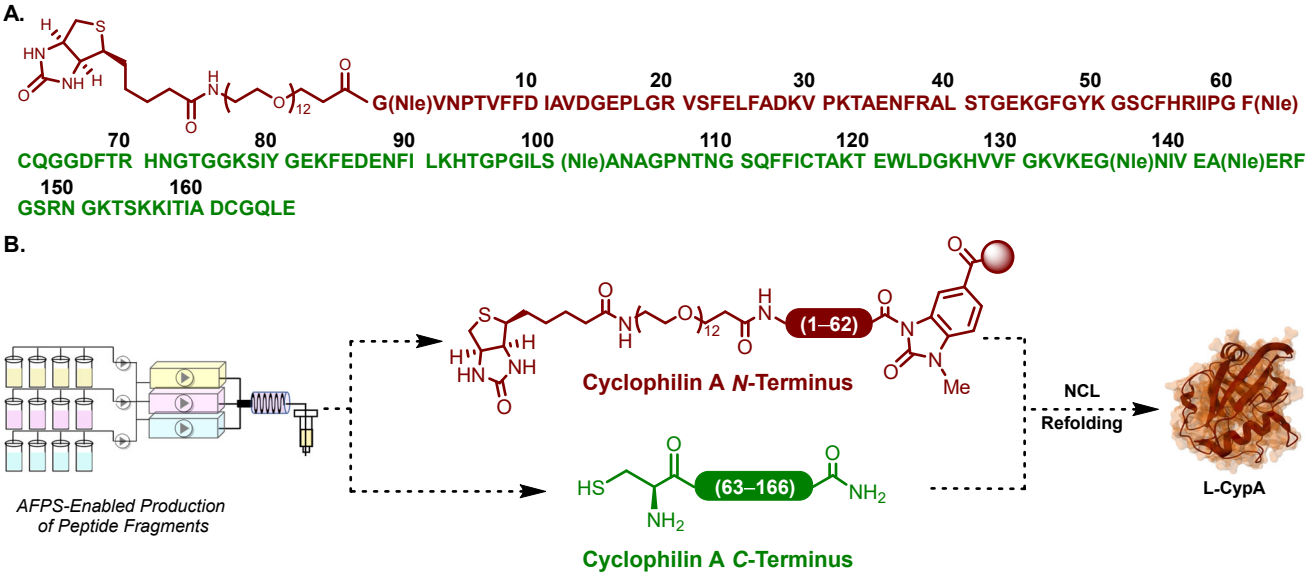


**Figure 2.** Automated fast-flow synthesis (AFPS) unveils rapid access to synthetic full-length CypA. **A.** Amino acid sequence of full-length CypA while methionine residues were replaced with norleucine. **B.** Proposed synthetic approach leveraging both AFPS and NCL methods for the production of full-length CypA. **C.** Shown are characterizations of CypA fragments, N-terminus (crimson) and C-Terminus (green), by RP-HPLC using UV detection at 214 nm, the mass-to-charge spectrum of the total ion current post-injection on a Q-TOF LC-MS instrument, and the deconvolution mass spectrum analysis (insets).

enabled the rapid optimization of the refolding strategy (Figure 3B).[34] After successfully obtaining the pellet containing the full-length ligated product of L-CypA, the synthetic protein was dissolved with a denaturing buffer containing 6 M Gmd•HCl with a concentration of 20 mg/mL and subsequently transferred to PCR tubes (200 μL). Various additives and buffers were added to these tubes to facilitate the refolding process. The resulting protein solutions with a concentration of 2.0 mg/mL were then incubated at 4 ºC for 16 hr before undergoing further analysis by DSF (see SI-Section 5 for details).

The overall trend from DSF experiments indicates that conditions involving the rapid dilution of Gmd•HCl lead to the formation of precipitates, regardless of the additives used (Figure 3B; Condition S12). Nevertheless, the presence of 1M Gmd•HCl in the refolding buffer aids in the proper folding of L-CypA (Figure 3B; Conditions S8, S9). It was hypothesized that the gradual removal of the denaturant is necessary for this challenging protein to establish essential non-covalent interactions within itself.[35] In line with this hypothesis, attempts involving serial dilution and on-column SEC folding of L-CypA resulted in the formation of aggregates exceeding 85% (Table 1, entries 1–2). Consequently, dialysis was employed to promote folding.[36] The SEC analysis of the refolding condition, utilizing the use of 3 MWCO dialysis cassettes and a refolding buffer containing 1.1 M Gdm•HCl, 55 mM Tris, 21 mM NaCl, 0.88 mM KCl, 10 mM DTT (pH 8.2) revealed the emergence of a new peak eluting at a similar time as the recombinant CypA protein (Table 1, entry 3). It was later found that the absence of Gdm•HCl in the refolding buffer drastically improves the refolding efficiency to 51% (entry 4). Additionally, using KPi buffer (57%, entry 5) for the refolding experiment was demonstrated to yield superior results. Efforts to enhance the efficiency of the refolding process by introducing additives such as salts, surfactants, and oligosaccharides which could avoid the formation of aggregates, did not significantly improve the outcome (<59% yield, entries 6–8).[37]

The scalability of the refolding reaction was demonstrated using a synthetic full-length L-CypA protein chain. Specifically, 2.1 mg of lyophilized powder containing L-CypA pellet was dissolved using a denaturing buffer to form a 5 μM protein

solution. Subsequently, the resulting solution was transferred into a dialysis cassette and dialyzed under Condition 5 (Table 1, entry 5) for 16 hr at 4 ºC. The dialyzed material is then purified

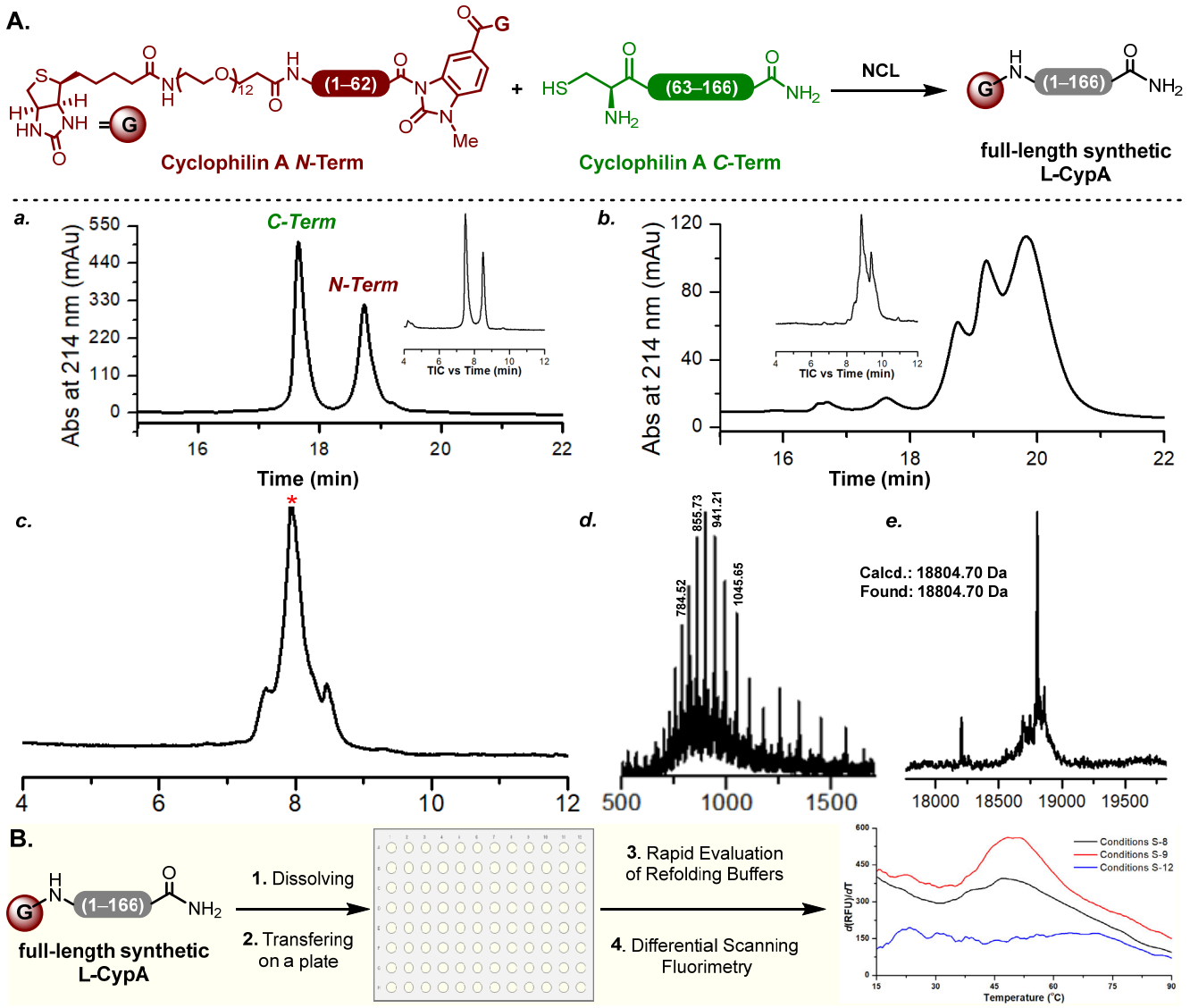


**Figure 3.** A single native chemical ligation enables the generation of synthetic full-length L-CypA. **A**. Monitoring NCL reaction by analytical RP-HPLC and LC-MS. RP-HPLC chromatogram and LC-MS analysis (inset) of NCL reaction at t = 1 min (***a.***), RP-HPLC chromatogram and LC-MS analysis (inset) of NCL reaction at t = 4 hr (***b.***), RP-HPLC chromatogram (***c.***), the mass-to-charge spectrum of the total ion current post-injection on a Q-TOF LC-MS instrument (***d.***), and the deconvolution mass spectrum analysis of the semi-purified NCL pellet (***e.***). **B.** Workflow for the rapid evaluation of refolding conditions by differential scanning fluorimetry (DSF) and corresponding thermal melting profiles of selected entries (**Condition S-8**: 1.1 M Gdm•HCl, 1.0 mM EDTA, 440 mM L-Arg, 55 mM Tris, 21 mM NaCl, 0.9 mM KCl, pH = 8.2; **Condition S-9**: 1.1 M Gdm•HCl, 1.0 mM EDTA, 880 mM L-Arg, 55 mM Tris, 21 mM NaCl, 0.9 mM KCl, pH = 8.2; **Condition S-12**: 880 mM L- Arg, 55 mM Tris, 21 mM NaCl, 0.9 mM KCl, pH =8.2 see supporting information for further details).

size exclusion chromatography to afford 77 μg folded protein (3.7% yield).

The quality of the synthetic folded L-CypA was validated using analytical RP-HPLC (Figure 4a), LC-MS (Figure 4b–c), and SEC (Figure 4h). To confirm that the biological activity of synthetic CypA matches that of recombinant protein, the binding affinity of both CypA proteins for cyclosporine A, a known binder of CypA, was examined using time-resolved fluorescence resonance energy transfer (TR-FRET). The study involved biotinylated recombinant and synthetic L-CypA, which were complexed with terbium-labeled streptavidin and then incubated with cyclosporine A, tagged with 4,4-difluoro-3a,4adiaza-s-indacene (BODIPY). The binding interaction was detected through an increase in fluorescence signal between the fluorophores (detailed in SI Section 7). The TR-FRET experiments indicated that the synthetic protein (KD = 80 ± 29 nM; Figure 4A.d) has a 2.8 times lower affinity for cyclosporine A than the recombinant version (KD = 29 ± 5 nM). Although it is still functional, the lower activity of the synthetic CypA might stem from the substitution of native methionine units with norleucine residues due to oxidation issues.[38]

The peptide-prolyl isomerase (PPI) activity of CypA, which involves the interconversion of the cis and trans isomers of proline residues within peptides, was successfully demonstrated for the synthetic proteins (Figure 4e).[1] Fischer and others described a colorimetric assay where chymotrypsin cleaves the

C-terminal amide bond of a model peptide, Suc-Ala-Ala-Pro-Phe-p-nitroanilide.[37-39] While the cis form of the model peptide is the dominant species at 22 ºC, it was found inactive towards hydrolysis.[39] On the other hand, the trans form rapidly undergoes chymotrypsin-mediated cleavage, releasing 4-nitroaniline that readily absorbs at 390 nm. In the assay, externally introduced

**Table 1.** Evaluation of folding conditions to generate functional full-length synthetic L-CypA.[a]

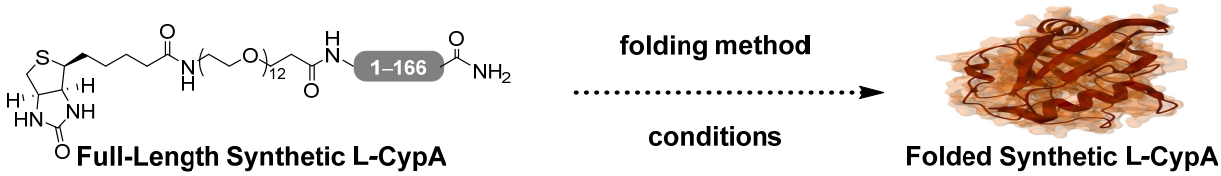


| Condition | Folding Method | Buffer Components | Additives | Folding Yield |
|---|---|---|---|---|
| 1[b] | Dilution | 1.1 M Gdm•HCl, 55 mM Tris, 21 mM NaCl, 0.88 mM KCl, pH = 8.2 | – | 13% |
| 2[c] | Size-Exchange Chromatography | 55 mM Tris, 21 mM NaCl, 0.88 mM KCl, pH = 8.2 | – | 15% |
| 3[d] | Dialysis | 1.1 M Gdm•HCl, 55 mM Tris, 21 mM NaCl, 0.88 mM KCl, 10 mM DTT, pH 8.2 | – | 29% |
| 4[d] | Dialysis | 100 mM Tris, 10 mM DTT, pH 8.2 | – | 51% |
| 5[d] | Dialysis | 100 mM KPi, 10 mM DTT, pH 8.2 | – | 57% |
| 6[d] | Dialysis | 100 mM KPi, 10 mM DTT, pH 8.2 | 200 mM NaCl | 43% |
| 7[d] | Dialysis | 100 mM KPi, 10 mM DTT, pH 8.2 | Triton X-100 2% (v/v) | 43% |
| 8[d] | Dialysis | 100 mM KPi, 10 mM DTT, pH 8.2 | β–cyclodextrin 230 μM | 59% |

Analytical SEC Analysis of Representative Entries

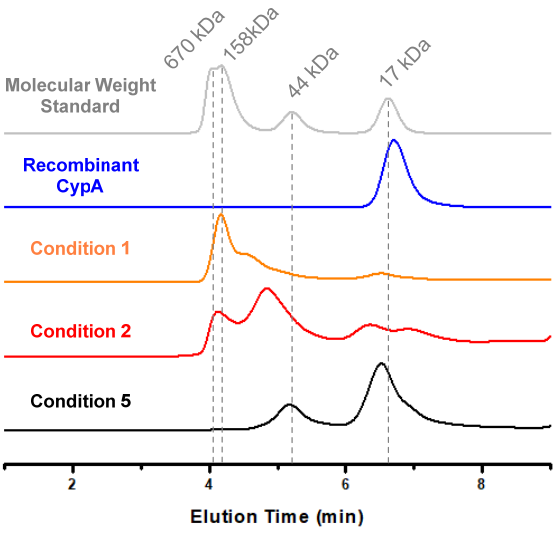


[a]Conditions: Synthetic L-CypA pellet (0.1–1 mmol) was dissolved in reductive denaturing buffer (6 M Gdm•HCl, 100 mM NaPi, 10 mM DTT, pH 8.0) to generate 20 μM protein solution. [b]The reduced protein (1–10 nmol) was then subjected to serial dilution (100x) with a buffer consisting of 1.1 M Gdm•HCl, 55 mM Tris, 21 mM NaCl, 0.88 mM KCl, pH = 8.2 to facilitate its refolding. [c]The reduced protein (1–10 nmol) was then directly injected into an SEC column and eluted with a refolding buffer (55 mM Tris, 21 mM NaCl, 0.88 mM KCl, pH = 8.2) to facilitate its refolding. [d]The reduced protein (1–10 nmol) was further diluted to 6 μM using the reductive denaturing buffer and was subsequently transferred to 3 kDa MWCO dialysis cassettes. The final solution was dialyzed against refolding buffers at 4 °C (2–16 h). For details, see the SI.

CypA is expected to promote the isomerization of peptide-prolyl bond, making the trans form available continuously, thereby increasing the observed rate of hydrolysis.

To prepare this assay, Suc-Ala-Ala-Pro-Phe-p-nitroanilide was dissolved in trifluoroethanol (TFE) containing 0.45 M LiCl to form a 16 mM peptide solution.[39,40] Meanwhile, a 60 mg/mL chymotrypsin solution in 1N HCl was prepared. The chymotrypsin solution and varied quantities of the synthetic L-CypA were mixed, further diluted with assay buffer, and allowed to incubate at 4 ºC for 10 minutes. Upon reaching thermal equilibrium, the peptide solution was rapidly mixed with the reaction solution, and the absorbance at 390 nm was immediately recorded. Despite a strong background reaction in the absence of a PPI, the results indicated that the addition of synthetic CypA significantly increased the reaction rate, demonstrating that the chemically synthesized protein exhibits functional properties.

The developed procedure for synthesizing functional full-length L-CypA was proved applicable for producing its mirror-image version, D-CypA. Accordingly, the AFPS-mediated synthesis of the C- and N-terminus of CypA was achieved while exclusively using mirror-image amino acid building blocks.[18,21–23,25,36] The resulting peptide chains were subjected to preparative RP-HPLC purification to afford purified C- (3.9% yield) and N-terminus (2.7% yield) fragments. Subsequently, the purified peptide chains were utilized in an NCL reaction affording full-length D-CypA pellet upon treating crude reaction mixture with prechilled water. Refolding the unpurified D-CypA pellet using Condition 5 generated folded mirror-image CypA (3.5% yield; Figure 4f–j). LC-MS (Figure 4f–g) chromatograms, analytical SEC (Figure 4h), and the SDS-PAGE gel (Figure 4i) of the D-CypA strictly bear a resemblance to those of synthetic L- and recombinant CypA. Further, the circular dichroism spectrum of D-CypA closely matches the inverted version of the spectra obtained for the synthetic L- and recombinant CypA (Figure 4j), consistent with the expectation that the folded conformation of the two proteins will be identical through the mirror plane.

## Conclusion:

In summary, the report presents the chemical synthesis of full-length Cyclophilin A proteins. By leveraging automated flow peptide synthesis, native chemical ligation techniques, and high-throughput evaluation of refolding conditions, we successfully obtained folded synthetic full-length L- and D-CypA proteins while minimizing the handling and purification steps that are required for conventional CSP. The confirmation of functionality was established through the cyclosporin binding and PPI assays.

Moreover, synthetically accessed full-length L- and D-CypA proteins hold the potential to serve as tools to identify novel probes, and ligands to inhibit numerous diseases, thereby opening up new possibilities for further research and applications in various fields.

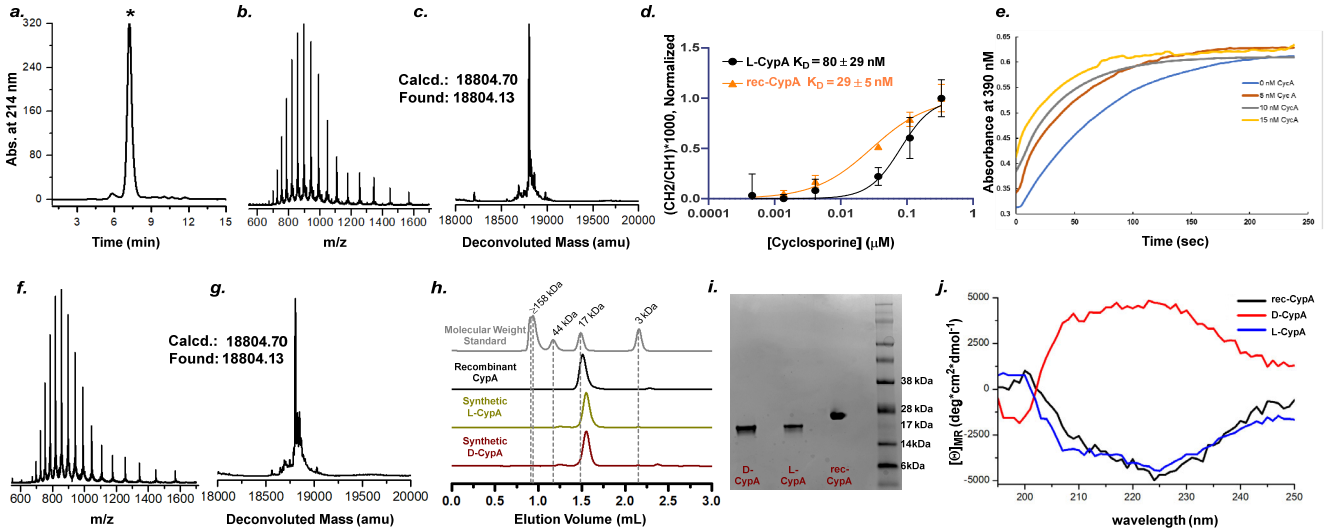


**Figure 4.** Analytical and biophysical characterization of folded synthetic full-length CypA proteins. Characterization of folded L-CypA: For the folded L-CypA characterization, the total ion current (TIC) chromatogram post-injection on a Q-TOF LC-MS instrument (***a***), the mass-to-charge spectrum of the total ion current (***b***), the deconvoluted mass spectrum (***c***), the TR-FRET binding assay (***d***) measuring FRET efficiency between BODIPY-labeled cyclosporin A (CspA) and terbium streptavidin that is attached to biotin-containing synthetic L- or rec-CycA proteins, and the results of the peptidylprolyl isomerase (PPIase) activity assay for synthetic L-CycA (***e***) were analyzed. For the folded D-CypA characterization, the mass-to-charge spectrum of the total ion current (***f***), the deconvoluted mass spectrum (***g***), analytical SEC of rec-CypA, synthetic L- and D-CypA using UV detection at 214 nm (***h***), SDS-PAGE gel of synthetic D- and L-CypA (MW: ≈18.8 kDa), and rec-CypA (MW: ≈21.5 kDa) (***i***), and circular dichroism spectra (***j***), which were recorded from 200 nm to 260 nm over a 0.1 cm pathlength at a protein concentration of 0.1 mg/mL using 50 mM KPi (pH 8.0) at 22 ˚C, were analyzed. The asterisk (*) in the TIC spectrum marks the primary product peak, corresponding to the integrated mass-to-charge and deconvoluted mass spectra shown in (***b***) and (***c***).

## Corresponding Authors

**Bradley L. Pentelute** − Department of Chemistry and Center for Environmental Health Sciences, Massachusetts Institute of Technology, Cambridge, Massachusetts 02139, United States; The Koch Institute for Integrative Cancer Research, Massachusetts Institute of Technology, Cambridge, Massachusetts 02142, United States; Broad Institute of MIT and Harvard, Cambridge, Massachusetts 02142, United States; orcid.org/0000-0002-7242-801X;

Email: blp@mit.edu

**John H. McGee** − FOG Pharmaceuticals Inc., 30 Acorn Park Drive, Cambridge, MA 02140, USA;

Email: jmcgee@fogpharma.com

## Acknowledgement

FOG Pharmaceuticals provided financial support for this work (to B.L.P.). We thank Giulio Fittolani for his valuable comments during manuscript preparation.

## Competing Interests

The authors declare the following competing interests: B.L.P. is a co-founder and/or member of the scientific advisory board of several companies focusing on the development of protein and peptide therapeutics. T.L.T, O.S.T., and J.H.M are currently employed by FOG Pharmaceuticals.

**Keywords**: flow synthesis • mirror-image proteins • native chemical ligation • protein folding • protein engineering • CypA

## References

(1) Nigro, P.; Pompilio, G.; Capogrossi, M. C. Cyclophilin A: A Key Player for Human Disease. Cell Death Dis. 2013, 4 (10), e888–e888. https://doi.org/10.1038/cddis.2013.410.

(2) Obchoei, S.; Wongkhan, S.; Wongkham, C.; Li, M.; Yao, Q.; Chen, C. Cyclophilin A: Potential Functions and Therapeutic. Med Sci Monit.

(3) Lee, J. Role of Cyclophilin a during Oncogenesis. Arch. Pharm. Res. 2010, 33 (2), 181–187. https://doi.org/10.1007/s12272-010-0200-y.

(4) Mamatis, J. E.; Pellizzari-Delano, I. E.; Gallardo-Flores, C. E.; Colpitts, C. C. Emerging Roles of Cyclophilin A in Regulating Viral Cloaking. Front. Microbiol. 2022, 13, 828078. https://doi.org/10.3389/fmicb.2022.828078.

(5) Padron, A.; Prakash, P.; Pandhare, J.; Luban, J.; Aiken, C.; Balasubramaniam, M.; Dash, C. Emerging Role of Cyclophilin A in HIV-1 Infection: From Producer Cell to the Target Cell Nucleus. J. Virol. 2023, 97 (11), e00732-23. https://doi.org/10.1128/jvi.00732-23.

(6) Matouschek, A.; Rospert, S.; Schmid, K.; Glick, B. S.; Schatz, G. Cyclophilin Catalyzes Protein Folding in Yeast Mitochondria. Proc. Natl. Acad. Sci. 1995, 92 (14), 6319–6323. https://doi.org/10.1073/pnas.92.14.6319.

(7) Dutta, D.; Barr, V. A.; Akpan, I.; Mittelstadt, P. R.; Singha, L. I.; Samelson, L. E.; Ashwell, J. D. Recruitment of Calcineurin to the TCR Positively Regulates T Cell Activation. Nat. Immunol. 2017, 18 (2), 196–204. https://doi.org/10.1038/ni.3640.

(8) Schulze, C. J.; Seamon, K. J.; Zhao, Y.; Yang, Y. C.; Cregg, J.; Kim, D.; Tomlinson, A.; Choy, T. J.; Wang, Z.; Sang, B.; Pourfarjam, Y.; Lucas, J.; Cuevas-Navarro, A.; Ayala-Santos, C.; Vides, A.; Li, C.; Marquez, A.; Zhong, M.; Vemulapalli, V.; Weller, C.; Gould, A.; Whalen, D. M.; Salvador, A.; Milin, A.; Saldajeno-Concar, M.; Dinglasan, N.; Chen, A.; Evans, J.; Knox, J. E.; Koltun, E. S.; Singh, M.; Nichols, R.; Wildes, D.; Gill, A. L.; Smith, J. A. M.; Lito, P. Chemical Remodeling of a Cellular Chaperone to Target the Active State of Mutant KRAS. Science 2023, 381 (6659), 794–799. https://doi.org/10.1126/science.adg9652.

(9) Holderfield, M.; Lee, B. J.; Jiang, J.; Tomlinson, A.; Seamon, K. J.; Mira, A.; Patrucco, E.; Goodhart, G.; Dilly, J.; Gindin, Y.; Dinglasan, N.; Wang, Y.; Lai, L. P.; Cai, S.; Jiang, L.; Nasholm, N.; Shifrin, N.; Blaj, C.; Shah, H.; Evans, J. W.; Montazer, N.; Lai, O.; Shi, J.; Ahler, E.; Quintana, E.; Chang, S.; Salvador, A.; Marquez, A.; Cregg, J.; Liu, Y.; Milin, A.; Chen, A.; Ziv, T. B.; Parsons, D.; Knox, J. E.; Klomp, J. E.; Roth, J.; Rees, M.; Ronan, M.; Cuevas-Navarro, A.; Hu, F.; Lito, P.; Santamaria, D.; Aguirre, A. J.; Waters, A. M.; Der, C. J.; Ambrogio, C.; Wang, Z.; Gill, A. L.; Koltun, E. S.; Smith, J. A. M.; Wildes, D.; Singh, M. Concurrent Inhibition of Oncogenic and Wild-Type RAS-GTP for Cancer Therapy. Nature 2024, 629 (8013), 919–926. https://doi.org/10.1038/s41586-024-07205-6.

(10) Tan, Y.; Wu, H.; Wei, T.; Li, X. Chemical Protein Synthesis: Advances, Challenges, and Outlooks. J. Am. Chem. Soc. 2020, 142 (48), 20288–20298. https://doi.org/10.1021/jacs.0c09664.

(11) Harel, O.; Jbara, M. Chemical Synthesis of Bioactive Proteins. Angew. Chem. Int. Ed. 2023, 62 (13), e202217716. https://doi.org/10.1002/anie.202217716.

(12) Borgia, J. A.; Fields, G. B. Chemical Synthesis of Proteins. 2000, 18.

(13) Nilsson, B. L.; Soellner, M. B.; Raines, R. T. Chemical Synthesis of Proteins. Annu. Rev. Biophys. Biomol. Struct. 2005, 34 (1), 91–118. https://doi.org/10.1146/annurev.biophys.34.040204.144700.

(14) Kent, S. B. H. Total Chemical Synthesis of Proteins. Chem Soc Rev 2009, 38 (2), 338–351. https://doi.org/10.1039/B700141J.

(15) Muir, T. W.; Kent, S. B. H. The Chemical Synthesis of Proteins.

(16) Hartrampf, N.; Saebi, A.; Poskus, M.; Gates, Z. P.; Callahan, A. J.; Cowfer, A. E.; Hanna, S.; Antilla, S.; Schissel, C. K.; Quartararo, A. J.; Ye, X.; Mijalis, A. J.; Simon, M. D.; Loas, A.; Liu, S.; Jessen, C.; Nielsen, T. E.; Pentelute, B. L. Synthesis of Proteins by Automated Flow Chemistry. 2020.

(17) Saebi, A.; Brown, J. S.; Marando, V. M.; Hartrampf, N.; Chumbler, N. M.; Hanna, S.; Poskus, M.; Loas, A.; Kiessling, L. L.; Hung, D. T.; Pentelute, B. L. Rapid Single-Shot Synthesis of the 214 Amino Acid-Long N-Terminal Domain of Pyocin S2. ACS Chem. Biol. 2023, 18 (3), 518–527. https://doi.org/10.1021/acschembio.2c00862.

(18) Xu, Y.; Zhu, T. F. Mirror-Image T7 Transcription of Chirally Inverted Ribosomal and Functional RNAs. Science 2022, 378 (6618), 405–412. https://doi.org/10.1126/science.abm0646.

(19) Williams, E. T.; Schiefelbein, K.; Schuster, M.; Ahmed, I. M. M.; De Vries, M.; Beveridge, R.; Zerbe, O.; Hartrampf, N. Rapid Flow-Based Synthesis of Post-Translationally Modified Peptides and Proteins: A Case Study on MYC's Transactivation Domain. Chem. Sci. 2024, 10.1039.D4SC00481G. https://doi.org/10.1039/D4SC00481G.

(20) Liu, M.; Pazgier, M.; Li, C.; Yuan, W.; Li, C.; Lu, W. A Left-Handed Solution to Peptide Inhibition of the P53–MDM2 Interaction. Angew. Chem. Int. Ed. 2010, 49 (21), 3649–3652. https://doi.org/10.1002/anie.201000329.

(21) Zhou, X.; Zuo, C.; Li, W.; Shi, W.; Zhou, X.; Wang, H.; Chen, S.; Du, J.; Chen, G.; Zhai, W.; Zhao, W.; Wu, Y.; Qi, Y.; Liu, L.; Gao, Y. A Novel D -Peptide Identified by Mirror-Image Phage Display Blocks TIGIT/PVR for Cancer Immunotherapy. Angew. Chem. Int. Ed. 2020, 59 (35), 15114–15118. https://doi.org/10.1002/anie.202002783.

(22) Callahan, A. J.; Gandhesiri, S.; Travaline, T. L.; Reja, R. M.; Lozano Salazar, L.; Hanna, S.; Lee, Y.-C.; Li, K.; Tokareva, O. S.; Swiecicki, J.-M.; Loas, A.; Verdine, G. L.; McGee, J. H.; Pentelute, B. L. Mirror-Image Ligand Discovery Enabled by Single-Shot Fast-Flow Synthesis of D-Proteins. Nat. Commun. 2024, 15 (1), 1813. https://doi.org/10.1038/s41467-024-45634-z.

(23) Harrison, K.; Mackay, A. S.; Kambanis, L.; Maxwell, J. W. C.; Payne, R. J. Synthesis and Applications of Mirror-Image Proteins. Nat. Rev. Chem. 2023, 7 (6), 383–404. https://doi.org/10.1038/s41570-023-00493-y.

(24) Kent, S. B. H. Novel Protein Science Enabled by Total Chemical Synthesis. Protein Sci. 2019, 28 (2), 313–328. https://doi.org/10.1002/pro.3533.

(25) Schumacher, T. N. M.; Mayr, L. M.; Minor, D. L.; Milhollen, M. A.; Burgess, M. W.; Kim, P. S. Identification of D -Peptide Ligands Through Mirror-Image Phage Display. Science 1996, 271 (5257), 1854–1857. https://doi.org/10.1126/science.271.5257.1854.

(26) Liang, X.; Kaya, A.; Zhang, Y.; Le, D. T.; Hua, D.; Gladyshev, V. N. Characterization of Methionine Oxidation and Methionine Sulfoxide Reduction Using Methionine-Rich Cysteine-Free Proteins. BMC Biochem. 2012, 13 (1), 21. https://doi.org/10.1186/1471-2091-13-21.

(27) Mergler, M.; Dick, F.; Sax, B.; Stähelin, C.; Vorherr, T. The Aspartimide Problem in Fmoc-based SPPS. Part II. J. Pept. Sci. 2003, 9 (8), 518–526. https://doi.org/10.1002/psc.473.

(28) Epand, R. M.; Raymer, K. E. Comparison of the Interaction of Methionine and Norleucine-containing Peptides with Phospholipid Bilayers. Int. J. Pept. Protein Res. 1987, 30 (4), 515–521. https://doi.org/10.1111/j.1399-3011.1987.tb03360.x.

(29) Fang, G.; Li, Y.; Shen, F.; Huang, Y.; Li, J.; Lin, Y.; Cui, H.; Liu, L. Protein Chemical Synthesis by Ligation of Peptide Hydrazides. Angew. Chem. Int. Ed. 2011, 50 (33), 7645–7649. https://doi.org/10.1002/anie.201100996.

(30) Blanco-Canosa, J. B.; Nardone, B.; Albericio, F.; Dawson, P. E. Chemical Protein Synthesis Using a Second-Generation N -Acylurea Linker for the Preparation of Peptide-Thioester Precursors. J. Am. Chem. Soc. 2015, 137 (22), 7197–7209. https://doi.org/10.1021/jacs.5b03504.

(31) Palomo, J. M. Solid-Phase Peptide Synthesis: An Overview Focused on the Preparation of Biologically Relevant Peptides. RSC Adv 2014, 4 (62), 32658–32672. https://doi.org/10.1039/C4RA02458C.

(32) Cistrone, P. A.; Bird, M. J.; Flood, D. T.; Silvestri, A. P.; Hintzen, J. C. J.; Thompson, D. A.; Dawson, P. E. Native Chemical Ligation of Peptides and Proteins. Curr. Protoc. Chem. Biol. 2019, 11 (1), e61. https://doi.org/10.1002/cpch.61.

(33) King, D. S.; Fields, C. G.; Fields, G. B. A Cleavage Method Which Minimizes Side Reactions Following Fmoc Solid Phase Peptide Synthesis. Int. J. Pept. Protein Res. 1990, 36 (3), 255–266. https://doi.org/10.1111/j.1399-3011.1990.tb00976.x.

(34) Biter, A. B.; De La Peña, A. H.; Thapar, R.; Lin, J. Z.; Phillips, K. J. DSF Guided Refolding As A Novel Method Of Protein Production. Sci. Rep. 2016, 6 (1), 18906. https://doi.org/10.1038/srep18906.

(35) Tsumoto, K.; Arakawa, T.; Chen, L. Step-Wise Refolding of Recombinant Proteins. Curr. Pharm. Biotechnol. 2010, 11 (3), 285–288. https://doi.org/10.2174/138920110791111979.

(36) Petersen, M. E.; Jacobsen, M. T.; Kay, M. S. Synthesis of Tumor Necrosis Factor α for Use as a Mirror-Image Phage Display Target. Org. Biomol. Chem. 2016, 14 (23), 5298–5303. https://doi.org/10.1039/C6OB00824K.

(37) Yamaguchi, H.; Miyazaki, M. Refolding Techniques for Recovering Biologically Active Recombinant Proteins from Inclusion Bodies. Biomolecules 2014, 4 (1), 235–251. https://doi.org/10.3390/biom4010235.

(38) Epand, R. M.; Raymer, K. E. Comparison of the Interaction of Methionine and Norleucine-containing Peptides with Phospholipid Bilayers. Int. J. Pept. Protein Res. 1987, 30 (4), 515–521. https://doi.org/10.1111/j.1399-3011.1987.tb03360.x.

(39) Xu, L.; Yan, X.; Luo, M.; Guan, Y.; Yao, S. Preparation, Characterization and Refolding in Vitro of a Recombinant Human Cyclophilin A Mutant: Effect of a Single Pro/Ser Substitution on Cyclophilin A Structure and Properties. Biotechnol. Prog. 2008, 24 (2), 302–310. https://doi.org/10.1021/bp070259m.

(40) Kofron, J. L.; Kuzmic, P.; Kishore, V.; Colon-Bonilla, E.; Rich, D. H. Determination of Kinetic Constants for Peptidyl Prolyl Cis-Trans Isomerases by an Improved Spectrophotometric Assay. Biochemistry 1991, 30 (25), 6127–6134. https://doi.org/10.1021/bi00239a007.